



Effects of different fat-suppression methods on T1 values in dynamic contrast-enhanced magnetic resonance imaging: a phantom study

Hiroyasu Ikeno¹ · Koji Sakai² · Hiroshi Imai³ · Masayoshi Mizuta⁴ · Toshiaki Nakagawa¹ · Mariko Goto² · Tsunao Kishida⁵ · Osam Mazda⁵ · Kei Yamada²

Received: 14 November 2018 / Revised: 20 June 2019 / Accepted: 26 June 2019 / Published online: 5 July 2019
© Japanese Society of Radiological Technology and Japan Society of Medical Physics 2019

Abstract

Dynamic contrast-enhanced MRI may yield variable longitudinal-relaxation time (T1) values depending on the precision of the fat-suppression (FS) technique. This study aimed to investigate the influences of FS methods on T1 value measurements on phantoms containing test tubes filled with mixtures of five volumes of fat, six amounts of contrast agent, and water. Volumetric interpolated images were obtained using several FS methods and flip angles. T1 maps were created based on the variable flip angle approach. The T1 values of water obtained by point-resolved single-voxel spectroscopy (SVS) were used as reference values. Notably, FS methods were shown to have substantial effects on the measurement of T1 values. Among the tested FS methods, the Dixon (water) method produced T1 values most similar to SVS, which can be considered as a reference value for clinical practice.

Keywords Dynamic contrast-enhanced magnetic resonance imaging · Fat-suppression · T1 value · Single voxel spectroscopy · Phantom

1 Introduction

Dynamic contrast-enhanced magnetic resonance imaging (DCE-MRI) has been used to observe various body parts. DCE-MRI of fat-abundant tissues, such as the breast, requires the use of a fat-suppression (FS) method to avoid unwanted high signals from fat tissue [1]. This method

enables stable observations of contrast enhancement within a fat-abundant environment.

Recently, the increased value of various quantitative parameter maps calculated from DCE-MRI has been reported not only for differential diagnoses, but also for assessments of the effects of treatment on malignant lesions [2]. Most of these quantitative parameters are calculated from non-contrast enhanced longitudinal-relaxation time (T1) maps and dynamic images after contrast administration [2].

For robustness, a guideline from the Quantitative Imaging Biomarkers Alliance (QIBA) recommends using variable flip angle (VFA) T1 mapping because this approach enables the operator to obtain a large area of a T1 map in a short time [3]. The guideline also recommends the use of the same pulse sequence and coils for both the T1 calculation and the DCE-MRI protocols. Accordingly, if FS is to be used in DCE-MRI, FS should be also applied to the scan used for the T1 calculation. However, QIBA has expressed concerns about the need for further investigation into the instability of FS methods, as it remains unclear whether FS methods can affect the calculation of a T1 value.

Several FS techniques are applicable to VFA T1 mapping, including chemical shift selective (CHESS) [4], spectral

✉ Hiroyasu Ikeno
ikeno@koto.kpu-m.ac.jp

¹ Department of Radiology, Kyoto Prefectural University of Medicine, 465 Kawaramachi-Hirokoji, Kamigyo-ku, Kyoto 602-8566, Japan

² Department of Radiology, Graduate School of Medical Science, Kyoto Prefectural University of Medicine, 465 Kawaramachi-Hirokoji, Kamigyo-ku, Kyoto 602-8566, Japan

³ MR Research and Collaboration Department, Siemens Healthcare K.K. Gate City Osaka West Tower 1-11-1 Osaka, Shinagawa-ku, Tokyo 141-8644, Japan

⁴ Department of Radiological Technology, Faculty of Medical Science, Kyoto College of Medical Science, 1-3 Imakita, Oyama-higashi, Sonobe, Nantan City, Kyoto 622-0041, Japan

⁵ Department of Immunology, Kyoto Prefectural University of Medicine, 465 Kawaramachi-Hirokoji, Kamigyo-ku, Kyoto 602-8566, Japan

attenuated inversion recovery (SPAIR) [5], Dixon [6], and water excitation (WE) [7]. The addition of the FS technique to a gradient echo (GRE) sequence changes the timing of pulse irradiation and may thus alter the signal intensity and T1 values. Furthermore, the different methods yield variable degrees of the FS effect due to differences in the frequency profile and sensitivity to static magnetic field inhomogeneity. Thus, the T1 values calculated from different FS methods may differ substantially.

In this study, we compared the effects of various FS methods on VFA T1 mapping using phantoms containing different fat fractions and contrast agent concentrations.

We applied inversion recovery-spin echo (IR-SE) [8] T1 mapping to a phantom without fat as the reference standard. Point-resolved single-voxel spectroscopy (SVS) was used as a reference to calculate the T1 value of the water-only component in the water-fat mixture phantom.

2 Materials and methods

2.1 Materials

All experiments were conducted using a clinical 3.0-T MRI scanner (Magnetom Skyra, version VE11C, Siemens Healthcare GmbH, Erlangen, Germany) with a 20-channel head-neck coil.

2.2 Phantoms

Solution phantoms with different fat contents and T1 values were prepared. Each mixture was enclosed in a 50-ml polypropylene screw-top test tube (inner diameter: 27.55 mm; length: 118 mm; ECK 50-mL self-supporting centrifuge tube; AS ONE, Co., Ltd., Osaka, Japan). Five fat concentrations (0, 5, 10, 20, 40 vol. %) were prepared using a water-soluble cutting oil (a mixture of 70–80% lubricant base oil, 1–5% triethanolamine, and an additive agent; AZ Co., Ltd., Osaka, Japan). The SVS spectrum of this oil contained two large peaks at 0.67 and 1.08 ppm (Fig. 1). Six concentrations of 38% meglumine gadoterate (Magnescope®, Guerbet Japan, Co., Tokyo, Japan) were used: 2.5, 1.3, 0.6, 0.3, 0.2, and 0.1 mM. These volumes were determined to yield T1 values of approximately 100–1500 ms in the nonfat solutions, as this range covers the T1 value ranges of a tumor before and after administration [9]. The 30 sample tubes were placed in two polypropylene containers (5-l capacity, size: 24 cm × 15 cm × 14 cm) and stabilized by tubes containing only tap water. One container held the 0, 5, or 10 vol. % fat content tubes, while the other contained the 20 or 40 vol. % tubes (Fig. 2a, b). An example of a T1 map created by IR-SE is shown in Fig. 2c. The spaces between the

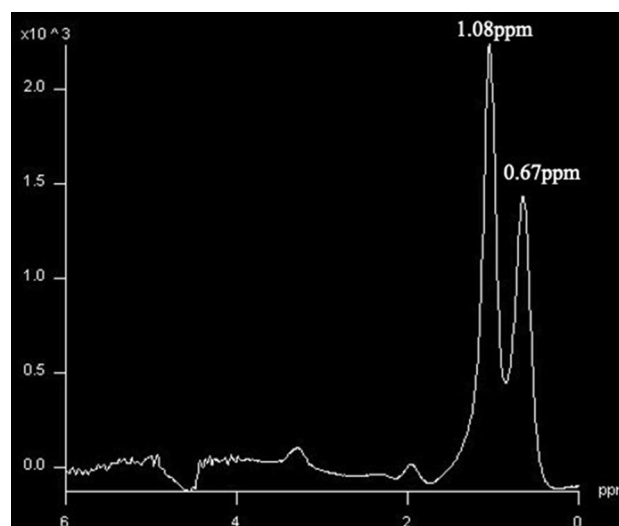


Fig. 1 A spectrum of water-soluble cutting oil

tubes and/or the container were filled with a 4.8 vol. % agar solution (Cool Agar®, Nitta Gelatin, Inc. Yabi City, Japan).

2.3 Acquisition and calculation of T1 values

The phantom was placed at the center of a receiver coil, and MR imaging was performed at room temperature (approximately 23 °C). Acquisitions for T1 calculations were performed using the following eight combinations: (1) VFA with GRE (VFA-off); (2) VFA with CHESS GRE (VFA-CHESS); (3) VFA with SPAIR GRE (VFA-SPAIR); (4) VFA with WE GRE (VFA-WE), which is a binominal expansion pulse obtained by dividing the flip angle into a 1:2:1 ratio; (5) VFA with in-phase GRE images [VFA-Dixon(in)], which was one of the dual-echo-time (TE) GRE images for the two-point Dixon method; (6) VFA with water images [VFA-Dixon(water)], which were calculated using the two-point Dixon method; (7) IR-SE; and (8) SVS. Among these, (2), (3), (4), (6), and (8) were used to calculate the T1 value only from the water component signal. Furthermore, (1), (5), and (7) were used to scan the samples without fat components.

The T1 map calculations for VFA and IR-SE were implemented using MATLAB® (The MathWorks, Inc., Natick, MA, USA). After selecting a center slice of the test tube, the mean and standard deviation were measured in the region of interest (ROI) that had been drawn manually on each tube using ImageJ (National Institutes of Health, Bethesda, Maryland, USA). For SVS, curve fitting was performed using the solver function of Excel 2011 (Microsoft Co., Redmond, WA, USA). The error ratio to the reference value was calculated from each calculated T1 value using this formula:

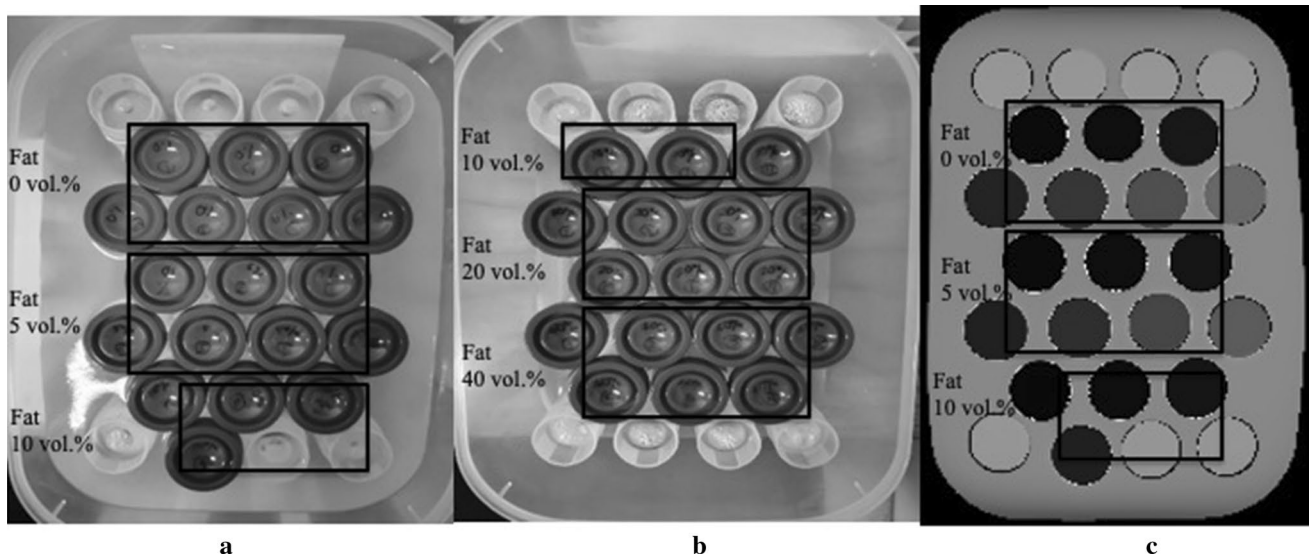


Fig. 2 **a** Photograph of a phantom with test tubes containing 50-ml solutions with fat concentrations of 0, 5, or 10 vol. %. **b** Photograph of a phantom with test tubes containing 50-ml solutions with fat concentrations at 10, 20, or 40 vol. %. **c** An example of a T1 map obtained using an MRI phantom

$$\frac{(T1\text{value calculated by each method}) - (T1\text{value calculated by SVS})}{T1\text{value calculated by SVS}} \times 100[\%]. \tag{1}$$

The imaging parameters for each method are shown in Table 1. Although the parameters in VFA should be identical except for FS, this was not possible due to system

restrictions. The details of each method are explained as follows.

Table 1 Imaging parameters for VFA gradient echo IR-SE and SVS sequences

VFA	IR-SE				SVS		
Fat-suppression	Off	CHESSE	SPAIR	WE	Dixon	Off	Off
Sequence	3D-VIBE		3D-VIBE		2D spin echo	Point resolved single voxel spectroscopy	
TR [ms]	20		20		10,000	200, 230, 250, 300, 350, 400, 600, 800, 1000, 1200, 1800, 2500, 3500, 5000, 7000, 10,000, 15,000	
TE [ms]	4.92		1.23, 2.46		8.5	33	
FA [degrees]	5, 12, 19, 26		5, 10, 15		90–180	90	
T1 [ms]	–		–		100, 300, 500, 750, 1000, 1500, 2000, 3000, 5000, 9000	–	
Slices	10		10		10	–	
FOV	250×250		300×300		250×250	15×15×30	
Thickness	3		3		8	–	
Matrix	320×320		160×160		256×256	–	
Average	1		1		1	5	
Parallel imaging	Off		Off		Off	–	
Band width [Hz/pixel]	300		1560, 1160		300	1200	

VFA variable flip angle, IR-SE inversion recovery-spin echo, SVS point resolved single voxel spectroscopy, CHESSE chemical shift selective, SPAIR spectral attenuated inversion recovery, WE water excitation, VIBE volumetric interpolated breath-hold examination

2.4 Variable flip angle gradient echo (VFA-GRE)

Two or more 3D-spoiled GRE acquisitions with identical parameters except for flip angles were performed for VFA T1 mapping. The theoretical formula of a spoiled GRE signal is:

$$S = M_0 \sin(\alpha) \frac{1 - \exp\left(-\frac{TR}{T_1}\right)}{1 - \cos(\alpha) \exp\left(-\frac{TR}{T_1}\right)} \quad (2)$$

This can be transformed to a linear equation as:

$$\frac{S}{\sin(\alpha)} = \exp\left(-\frac{TR}{T_1}\right) \frac{S}{\tan(\alpha)} + M_0 \left\{ 1 - \exp\left(-\frac{TR}{T_1}\right) \right\}, \quad (3)$$

Where S is the signal on a pixel, α is the flip angle, TR is the repetition time, and M_0 is the equilibrium magnetization. The T1 value can be determined from this equation by linear fitting. In VFA, phantoms with various T1 values are measured simultaneously. Three FAs were used for Dixon, while four FAs were used for the other FS methods because the optimal FA differs for each phantom [10]. As a B1 + map was required for the correction to an effective flip angle, B1 + mapping was performed via the preconditioning pulse method [11], which enabled the determination of many slices of a B1 + map within a short period. The scan parameters were as follows: field of view (FOV) = 300 mm, slice thickness = 8 mm, matrix size = 64 × 64, TR = 5280 ms, TE = 1.83 ms, FA = 8°, bandwidth = 490 Hz/pixel.

2.5 Inversion recovery spin echo (IR-SE)

During IR-SE T1 mapping, imaging was performed by changing only the inversion time (TI). T1 maps were created by nonlinear curve fitting, based on the following theoretical equation for the signals obtained from each pixel:

$$S = M_0 \left(1 - 2 \exp\left(-\frac{TR}{T_1}\right) \right). \quad (4)$$

This method was applied only to samples without fat because the FS technique was not applied.

2.6 Point-resolved single-voxel spectroscopy (SVS) sequence

SVS enables evaluation of the signal from the water component without any effect from the fat component. We, therefore, used this sequence as a reference for the water component T1 value in a water-fat mixture. The SVS signals for each sample were acquired consecutively while changing

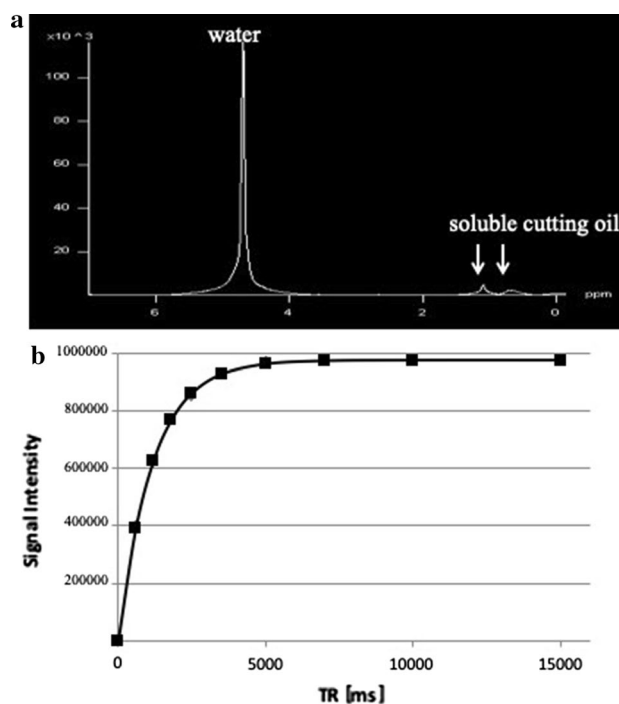


Fig. 3 Scheme of water-fat MR spectroscopy: **a** an example of chemical shift relative to the frequency, **b** relationship between signal intensities and TR in the phantom containing 20 vol. % fat and 2.5 mM contrast agent. T1 values of the water component were evaluated from SVS with variable TRs (200–15,000 ms). T1 values were calculated from the plotted signals of SVS at several TRs

the TR and retaining other scan parameters and adjustments (e.g., transmitter, shimming, and water suppression). Post-processing was performed using the Syngo (Siemens Healthcare GmbH, Erlangen, Germany) Spectroscopy tool on the system console. The spectrum of the water component was fitted using a Lorentzian curve after conducting Hanning filter processing, zero-filling, Fourier transformation, baseline correction, and phase correction. Next, the area under the curve (AUC) was measured (Fig. 3a). All processes were performed automatically to avoid arbitrariness. However, manual adjustments were performed by a radiological technologist with more than 9 years of experience in MR imaging only when these changes clearly improved the fitting accuracy. The T1 values of each sample were calculated by nonlinear curve fitting for the AUCs of each TR, using the following equation (Fig. 3b):

$$S = M_0 \left(1 - \exp\left(-\frac{TR}{T_1}\right) \right), \quad (5)$$

Where M_0 represents the AUC at a TR where longitudinal magnetization was completely recovered.

Fig. 4 Relationship between 1/T1 and the concentration of contrast agent in 8 different imaging sequences in samples without fat (fat content: 0 vol. %)

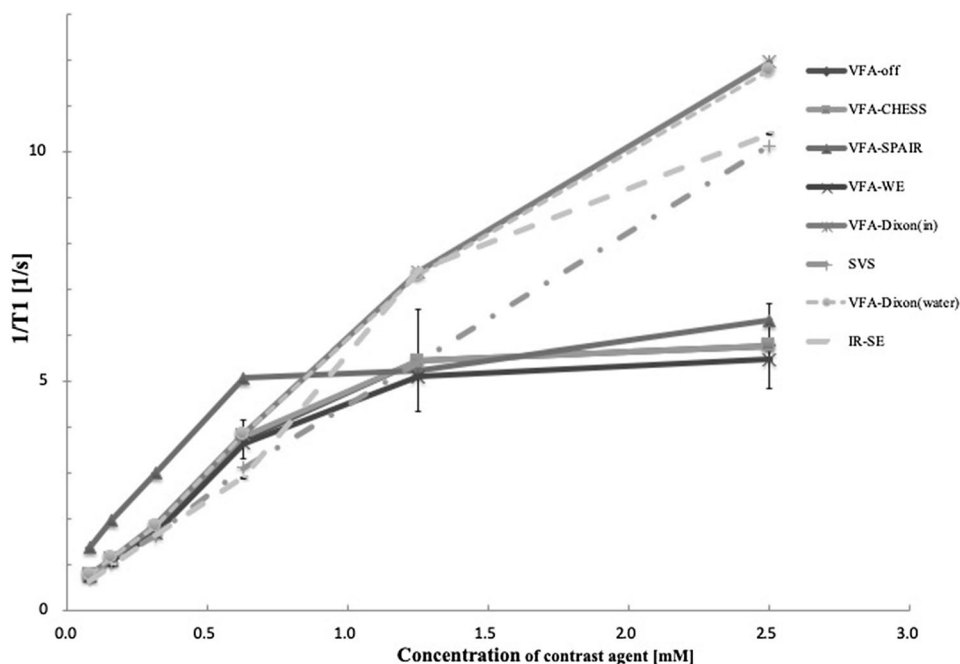
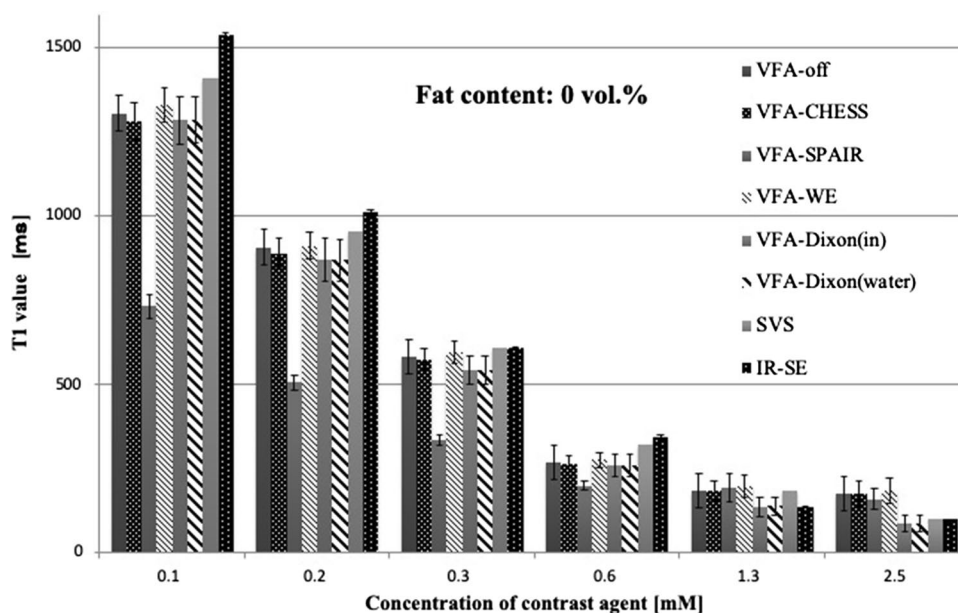


Fig. 5 Relationship between T1 and the concentration of contrast agent in 8 different imaging sequences in samples without fat (fat content: 0 vol. %)



3 Results

Figure 4 depicts the relationship between the concentration of contrast agent and the 1/T1 of solutions with a fat content of 0 vol. %. VFA-Dixon(in) and VFA-Dixon(water) exhibited tendencies similar to the reference methods of IR-SE and SVS, whereas other methods tended to yield underestimations under high concentrations of contrast agent. Figure 5 shows the relationship between the T1 values and the amount of contrast agent. Solutions with a low concentration of contrast agent (0.1 mM) yielded the greatest difference

between the reference SVS and VFA-SPAIR sequences (−48.3%). The differences obtained with the other methods were as follows: VFA-off: −7.5%, VFA-CHES: −9.2%, VFA-WE: −5.7%, VFA-Dixon(in): −9.0%, VFA-Dixon(water): −8.9%, and IR-SE: 5.6%. In the sample with the highest concentration of contrast agent (2.5 mM), values similar to the reference SVS were obtained using IR-SE (−7.2%), VFA-Dixon(in) (−15.4%), and VFA-Dixon(water) (−14.0%); the other results were VFA-off: 75.5%, VFA-CHES: 75.6%, VFA-SPAIR: 60.3%, and VFA-WE: 85.0%.

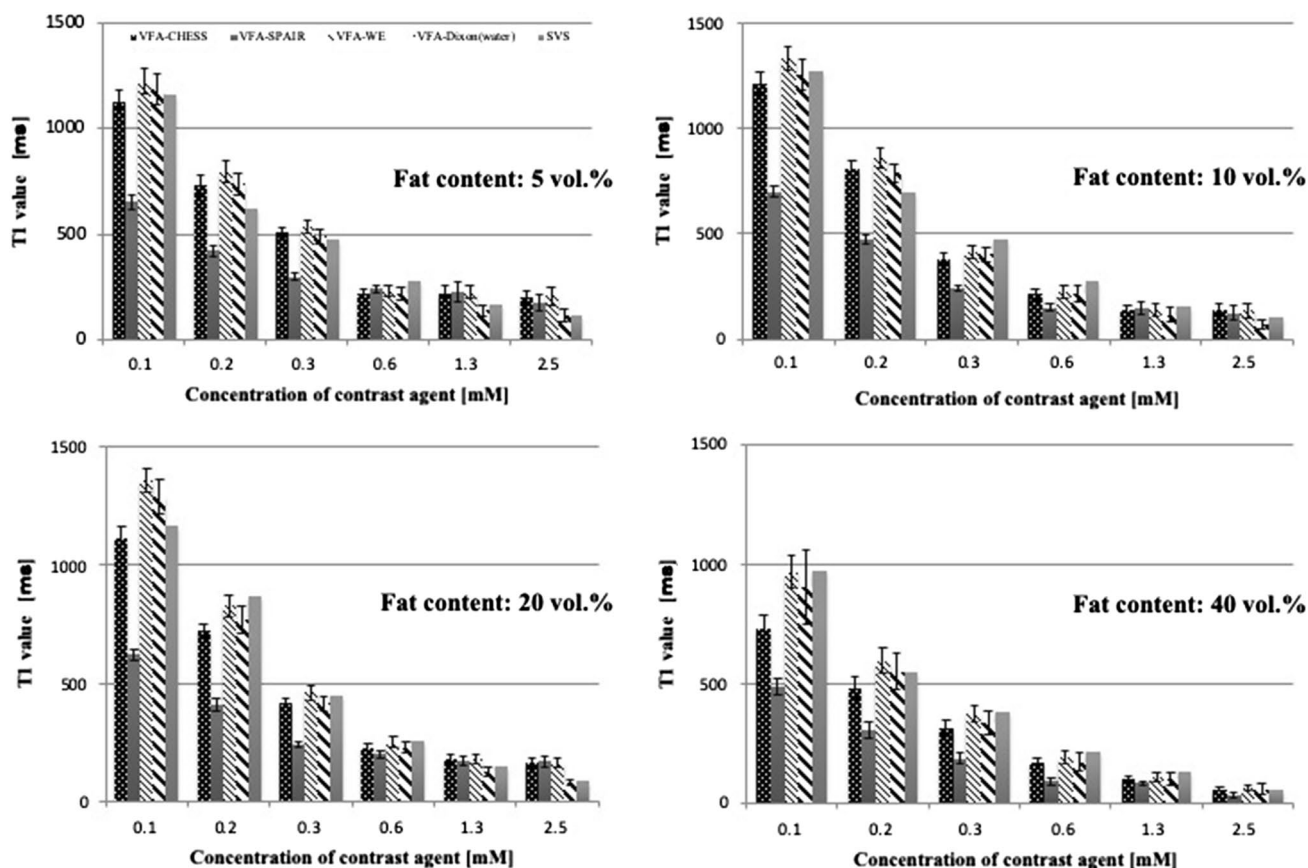


Fig. 6 Relationship between T1 and the concentration of contrast agent in five different imaging sequences in samples without fat contents (5, 10, 20, or 40 vol. %)

Figure 6 presents the T1 values of the four FS techniques and the reference SVS with different amounts of fat content. The T1 values of VFA-SPAIR yielded the greatest difference when compared with SVS (Fig. 6). Of the four FS techniques, the T1 values of VFA-Dixon(water) were the most similar to those of SVS, irrespective of the concentration of contrast agent (Table 2).

4 Discussion

In this study, we demonstrated that the T1 values obtained using VFA varied with the FS method of choice, even when a nonfat phantom was scanned. Regardless of the fat content, the SPAIR method yielded the greatest variation of T1 values from the reference SVS, whereas the Dixon(water) method yielded the least difference from the reference.

In almost all phantoms with a fat component, the T1 values obtained with Dixon(water) were most similar to those of SVS, irrespective of the amount of fat (Fig. 6, Table 2).

This is attributed to filling of the k-space with steady-state signals, given the lesser effect from the FS pulses applied on the TR intervals. In contrast, the T1 values obtained with SPAIR were significantly lower than those of SVS, irrespective of the amount of fat (Fig. 6, Table 2). In particular, the T1 values of SPAIR exhibited the greatest differences from SVS of all tested FS methods. This is attributed to a prolongation of the time to a state of thermal equilibrium due to the large FA. An effective FS method should exclude the effect of the present fat tissue from the T1 value, regardless of the fat content. However, our results demonstrated differences between the T1 values of the fat contents in the 5 and 40 vol. % sample tubes.

Our results are in accordance with those reported by Houchun et al. [12], who demonstrated that the presence of fat itself shortened the T1 values of water. In our study, the sample tubes without fat also exhibited different T1 values when subjected to different FS methods. The trend of Dixon(water) was the closest to SVS, whereas the other FS methods exhibited differing trends from SVS, especially

Table 2 Ratios of VFA-CHESS, VFA-SPAIR, VFA-WE, and VFA-Dixon(water) to the reference SVS at five different fat contents and two different contrast agent concentrations

Fat content [vol. %]	Concentration of contrast agent [mM]	VFA-CHESS	VFA-SPAIR	VFA-WE	VFA-Dixon (water) [%]
0	0.1	-9.2	-48.3	-5.7	-8.9
	2.5	75.6	60.3	85.0	-14.0
5	0.1	-3.1	-43.9	5.2	1.8
	2.5	78.1	55.8	82.5	2.1
10	0.1	-4.7	-45.2	4.3	-1.6
	2.25	37.3	25.2	34.9	-29.0
20	0.1	-4.3	-46.7	16.7	10.5
	2.5	83.5	91.5	88.1	-7.3
40	0.1	-24.9	-49.9	-0.2	-7.0
	2.5	4.9	-41.9	12.4	5.1
Average \pm SD	0.1	-9.3 \pm 10.5	-46.4 \pm 2.6	6.5 \pm 7.2	0.9 \pm 7.3
	2.5	51.0 \pm 37.0	32.7 \pm 56.6	54.5 \pm 36.8	-7.3 \pm 15.4

VFA variable flip angle, SVS point resolved single voxel spectroscopy, CHESS chemical shift selective, SPAIR spectral attenuated inversion recovery, WE water excitation

at high concentrations of contrast agent (Fig. 4). SPAIR yielded underestimation rates of 48.3% at a contrast agent concentration of 0.1 mM and 60.6% at 2.5 mM and exhibited the greatest differences from SVS and IR-SE (references) of all tested FS methods (Fig. 5, Table 2). We speculate that these differences were attributable to the collapse of the steady state by the FS pulses. Generally, GRE sequences are used for VFA. As mentioned above, GRE sequences fill the k-space with stable signals at the steady state by applying repeated radio frequency (RF) pulses of the same FA with a short TR [13]. However, SPAIR and CHESS sequences do not acquire a signal in the steady state when a FS pulse is applied every several TRs. In the present study, one FS pulse was applied to every 20-slice encoding, and each application corresponded to a steady state collapse. Although a signal was acquired when fat recovered to the null point, this signal was probably unstable and had not yet reached a steady state. Therefore, we considered the k-space to have been filled with non-steady-state signals, which probably affected the T1 value after image reconstruction.

According to previous work, at a subject T1 value greater than 900 ms, a difference of more than 15% with respect to the theoretical value could be observed by the use of a 3D fast low angle shot (FLASH) with VFA. This difference was speculated to occur because of incomplete spoiling and an imperfect FA [14]. When using our phantoms, which yielded T1 values exceeding 900 ms with SVS (contrast agent concentration = 0.1 mM), differences exceeding 15% were observed relative to SVS for VFA-CHESS (fat content: 40 vol. %), VFA-SPAIR (fat content: 5, 10, 20, and 40 vol. %), and VFA-WE (fat content: 20 vol. %). However, the T1 values obtained using VFA-Dixon(water) exhibited a difference

of less than 15%. In breast tumors, the T1 value may exceed 900 ms [9]; therefore, we believe that the Dixon(water) is one of the best FS options for DCE-MRI.

This study had some limitations. First, the fat component of the water-soluble cutting oil used in the current experiment differed from actual human fat and exhibited only two peaks in the chemical shift spectrum at 1.08 and 0.67 ppm (Fig. 3). In contrast, the human fat spectrum contains many peaks corresponding to chemical shifts, some of which can be observed near the water peak when using high-field MR units [15]. The FS pulse width of SPAIR is 440 Hz, and the edge of the pulse is 255 Hz away from the central frequency of water. Therefore, the FS pulse of SPAIR may reduce fat signal suppression near the water peak in human subjects. In addition, both the in-phase and opposed-phase of the Dixon method were designed to fit the difference in frequencies between water and fat in the human body. Furthermore, the user cannot change the frequency settings for Dixon on the MRI console. Therefore, the Dixon(water) images obtained of our phantoms may differ from those obtained from a human subject.

5 Conclusion

FS methods have substantial effects on measured T1 values. We conclude that Dixon(water) is among the best FS methods for the accurate quantitative evaluation of T1 values during DCE-MRI.

The authors certify that they have no actual or potential conflicts of interest in relation to this article.

Compliance with ethical standards

Ethical approval This article does not contain any studies or experiments performed by any of the authors on human participants or animals.

References

1. D'Orsi C, Sickles E, Mendelson E, Morris E. ACR BI-RADS Atlas, breast imaging reporting and data system. 5th ed. Reston: American College of Radiology; 2013.
2. Tofts P. T1-weighted DCE imaging concepts: modeling, acquisition and analysis. *Siemens Magn Flash*. 2010;3:31–9.
3. Profile: DCE MRI Quantification. version 1.6. RSNA 2011: 8-13, 35-46.
4. Haase A, Frahm J, Hänicke W, Matthaei D. 1H NMR chemical shift selective (CHESS) imaging. *Phys Med Biol*. 1985;30(4):341–4.
5. Tannus A, Garwood M. Adiabatic pulses. *NMR Biomed*. 1997;10:423–43.
6. Dixon W. Simple proton spectroscopic imaging. *Radiology*. 1984;153:189–94.
7. Schick F, Forster J, Machann J, Huppert P, Claussen C. Highly selective water and fat imaging applying multislice sequences without sensitivity to B1 field inhomogeneities. *Magn Reson Med*. 1997;38:269–74.
8. Timothy R, Mikulis D. Neuro MR: principles. *J Magn Reson*. 2007;2(6.4):823–37.
9. Takezawa K, Goto M, Sakai K, Ikeno H, Nakatsukasa K, Imai H, and Yamada K. Influence of FS to evaluate T1 values in breast cancer: assessing the reliability of pharmacokinetic parameters[Abstract]. Proceedings of the 23th Annual Meeting of the international Society for Magnetic Resonance in Medicine, 30 May – 5 June 2015.
10. Wang H, Riederer S, Lee J. Optimizing the precision in T1 relaxation estimation using limited flip angles. *Magn Reson Med*. 1987;5:399–416.
11. Chung S, Kim D, Breton E, Axel L. Rapid B1 + mapping using a preconditioning RF pulse with TurboFLASH readout. *Magn Reson Med*. 2010;64:439–46.
12. Hu HH, Nayak KS. Change in the proton T1 of fat and water in mixture. *Magn Reson Med*. 2010;63:494–501.
13. Araki T. Complete explanation of MRI, 2nd Edition, Gakken Medical Shujunsya, Co; 2014. p. 239-247 (in Japanese).
14. Brookes JA, Redpath TW, Gilbert FJ, Needham G, Murray AD. Measurement of spin-lattice relaxation times with FLASH for dynamic MRI of the breast. *Br J Radiol*. 1996;69:206–14.
15. Ren J, Dimitrov I, Sherry AD, Malloy CR. Composition of adipose tissue and marrow fat in humans by 1H NMR at 7 tesla. *J Lipid Res*. 2008;49:2055–62.

Publisher's Note Springer Nature remains neutral with regard to jurisdictional claims in published maps and institutional affiliations.